Transient Analyses of Grounding Electrodes Considering Ionization and Dispersion Aspects of Soils Simultaneously: An Improved Multiconductor Transmission Line Model (Improved MTL)

Seyyed Sajjad Sajjadi, Vahid Aghajani, and Saeed Reza Ostadzadeh

Department of Engineering, Arak University, Arak, Iran
sajadi-elek@gmail.com, v-aghajani@msc.araku.ac.ir, s-ostadzadeh@araku.ac.ir

Abstract **─** This paper proposes an approximate model in the frequency domain for transient analysis of grounding electrodes buried in ionized and dispersive soils. The proposed method, called multi-conductor transmission line model (MTL), can easily treat the frequency dependence of electrical parameters of soil. It can also incorporate soil ionization by gradually changing the respective electrode radius. Extensive simulation results are presented to confirm the accuracy of the MTL.

Index Terms **─** Frequency dependence, ionization, multi-conductor transmission lines.

I. INTRODUCTION

The lightning performance of grounding systems plays a significant role in the safe and reliable operation of power networks [1, 2]. A grounding system, including buried horizontal electrodes, vertical rods and grounding grids, is designed to effectively dissipate large lightning surge currents into the soil, ensuring reduced grounding impedance. Such a provision prevents the generation of catastrophic overvoltage that could cause transmission line outages and equipment damages.

A proper design of a grounding system requires an efficient method for transient analysis of grounding electrodes buried in the ground, considering soil ionization and dispersion. The former arises when the lightning voltage on a rod exceeds the soil voltage breakdown, while the latter is due to the frequency dependence of electrical parameters of soil. A solution of the problem considering solely the nonlinear effect of soil ionization can be sought through the use of time-domain [3-5], frequency-domain [6-8], and hybrid time-frequency domain [9-13] methods. In the cases where soil dispersion is occurred, the frequency-domain techniques such as the method of moments (MoM) [14], the finite element method (FEM) [15], and the hybrid electromagnetic-method (HEM) [16] becomes more noticeable. For a comprehensive analysis of grounding systems, considering both the dispersion and ionization of soil, several hybrid time-frequency domain methods have been proposed. These include a combined FEM in the spatial domain with the finite difference time domain (FDTD) [9] and combined frequency-domain numerical techniques and circuit theory [10-13].

Despite the accuracy of the numerical methods mentioned above, they are generally less efficient than the so-called analytical solutions where the full wave analysis is approximated by using appropriate lumped circuit elements [17, 18] or assuming transverse electromagnetic (TEM) wave propagation along grounding conductors [19]. Although these methods are more appealing for their many features, including the generality of the solution in the form of closed mathematical relations and relatively fewer computation resources, these methods suffer from a number of drawbacks: a) soil ionization is included through a nonlinear conductance which is restricted to lengths less than 30m [20], and b) the couplings between conductors are ignored. Although improved transmission line model [21] and non-uniform transmission line model [22] were later proposed to consider mutual coupling between conductors in the grounding grid, they are combined with time-consuming numerical methods such as FEM and FDTD respectively.

In a recent work [23], these shortcomings have been resolved by considering each set of parallel conductors in the grounding grid as a multi-conductor transmission lines (MTL). A two-port network for each set of parallel conductors in the grid is then defined. Finally, the two-port networks are interconnected depending upon the pattern of connections in the grid and its representative equations then reduced. Through this approach, voltages and currents at any junction in the grid is easily extracted. Application of this modeling approach in analyzing grounding grids buried in soils with constant electrical parameters was investigated. Also, since it is in the frequency domain, it can be evidently used in soils with frequency-dependent electrical parameters. Hence in this paper it is improved to consider soil ionization by gradually changing the respective electrode radius. The simplicity and computation efficiency of the method

Submitted On: September 26, 2018
Accepted On: February 9, 2019

make it advantageous over the exact methods while being able to consider all practical characteristics such as ionization and dispersion of soils separately or simultaneously.

This paper is organized as follows. In Section II, the improved MTL approach is completely explained. In Section III, model evaluation and efficiency in transient analyses of grounding systems buried in dispersive and ionized soils separately and simultaneously is investigated. Finally concluding remarks are given in Section IV.

II. MODELING APPROACH

To extract MTL approach, at first assume single transmission line of length l as shown in Fig. 1 (a). The following set of equations describing the propagation phenomenon in this transmission line is as below:

$$-\frac{d^2}{dx^2}V = ZYV = PV, \tag{1}$$

$$-\frac{d^2}{dx^2}I = YZI = P_t V, \tag{2}$$

where Z and Y represent, respectively, the series impedance and parallel admittance per unit length, I and V are respectively, the phasor of current and voltage with respect to a point at infinite as shown in Fig. 1 (a). In addition, $P = ZY$, $P_t = YZ$ and x is the variable of length.

Applying a linear transformation in order to diagonalize P and P_t, solutions to (1) and (2) can be expressed as follows:

$$I_s = Y_0 \coth(\Psi l)V_s - Y_0 \operatorname{csch}(\Psi l)V_r, \tag{3}$$

$$I_r = -Y_0 \operatorname{csch}(\Psi l)V_s + Y_0 \coth(\Psi l)V_r. \tag{4}$$

Rewriting (3) and (4) in matrix form, we have:

$$\begin{bmatrix} I_s \\ I_r \end{bmatrix} = \begin{bmatrix} A & B \\ C & D \end{bmatrix} \begin{bmatrix} V_s \\ V_r \end{bmatrix}, \tag{5}$$

where $A = D = Y_0 \coth(\Psi l)$ and $B = C = -Y_0 \operatorname{csch}(\Psi l)$. V_s and I_s represent, respectively, the voltage and current at the sending end of the line, and V_r and I_r are, respectively, the voltage and current at the receiving end of the line. Also, ψ and l denote the propagation constant and length of transmission line respectively. Using (5), relation between sending and receiving currents and voltages for a conductor of length l can be represented as a two-port network as shown in Fig. 1 (b).

Now, consider a mesh 1×1 as shown in Fig. 2. In this figure, two pairs of parallel conductors are seen, i.e., (1-2) and (2-4) which are mutually coupled. As a result, the relation (5) is extended as (6) and (7) respectively for pairs (1-3) and (2-4),

$$\begin{bmatrix} I_{s1} \\ I_{s3} \\ I_{r1} \\ I_{r3} \end{bmatrix} = \begin{bmatrix} A_{11} & A_{12} & B_{11} & B_{12} \\ A_{21} & A_{22} & B_{21} & B_{22} \\ C_{11} & C_{12} & D_{11} & D_{12} \\ C_{21} & C_{22} & D_{21} & D_{22} \end{bmatrix} \begin{bmatrix} V_{s1} \\ V_{s3} \\ V_{r1} \\ V_{r3} \end{bmatrix}, \tag{6}$$

$$\begin{bmatrix} I_{s2} \\ I_{s4} \\ I_{r2} \\ I_{r4} \end{bmatrix} = \begin{bmatrix} A_{11} & A_{12} & B_{11} & B_{12} \\ A_{21} & A_{22} & B_{21} & B_{22} \\ C_{11} & C_{12} & D_{11} & D_{12} \\ C_{21} & C_{22} & D_{21} & D_{22} \end{bmatrix} \begin{bmatrix} V_{s2} \\ V_{s4} \\ V_{r2} \\ V_{r4} \end{bmatrix}. \tag{7}$$

According to (6) and (7), the two-port network in Fig. 1 (b) is generalized as shown in Fig. 3.

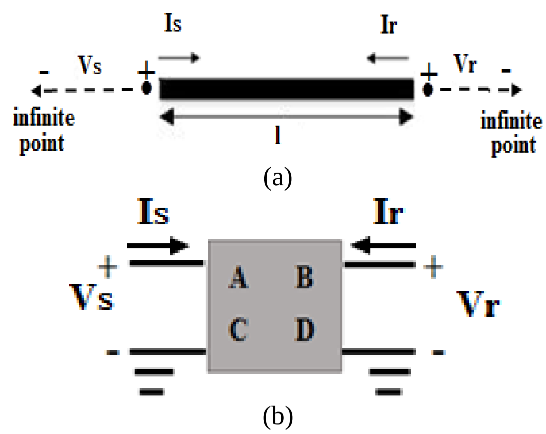

Fig. 1. (a) A conductor of length 1 with definition of voltage and current at sending and receiving points, and (b) representation of the conductor as a two-port network.

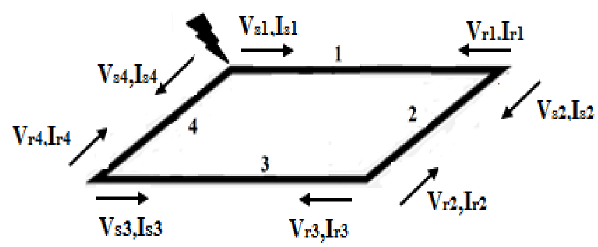

Fig. 2. Mesh 1×1 consisting of two pairs of parallel conductors.

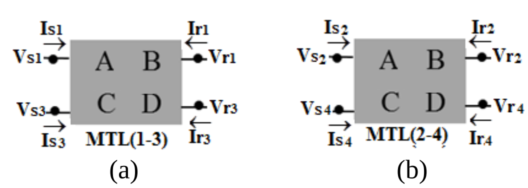

Fig. 3. Representation of two-port network for: (a) MTL (1-3), and (b) MTL (2-4) considering mutual coupling effect.

Due to mesh connections in Fig. 2, the two MTLs in Fig. 3 are connected as shown in Fig. 4. The relations (6) and (7) can be incorporated in a following matrix form:

$$\bar{I} = \overline{\overline{MTL}} \times \bar{V}, \tag{8}$$

where

$$\bar{I} = \begin{bmatrix} I_{s1} & I_{s2} & I_{r1} & I_{r3} & I_{s2} & I_{s4} & I_{r2} & I_{r4} \end{bmatrix}^T, \tag{9}$$

$$\bar{V} = \begin{bmatrix} V_{s1} & V_{s3} & V_{r1} & V_{r3} & V_{s2} & V_{s4} & V_{r2} & V_{r4} \end{bmatrix}^T, \tag{10}$$

$$\overline{\overline{MTL}} = \begin{bmatrix} A_{11} & A_{12} & B_{11} & B_{12} & & & & \\ A_{21} & A_{22} & B_{21} & B_{22} & & 0 & & \\ C_{11} & C_{12} & D_{11} & D_{12} & & & & \\ C_{21} & C_{22} & D_{21} & D_{22} & & & & \\ & & & & A_{11} & A_{12} & B_{11} & B_{12} \\ & & & & A_{21} & A_{22} & B_{21} & B_{22} \\ & 0 & & & C_{11} & C_{12} & D_{11} & D_{12} \\ & & & & C_{21} & C_{22} & D_{21} & D_{22} \end{bmatrix}. \tag{11}$$

It should be noted that in (11), mutual coupling between parallel conductors in the grid is completely included. In the cases of vertical rods, and horizontal electrodes, more elements of (11) are zero, because there is no parallel conductor.

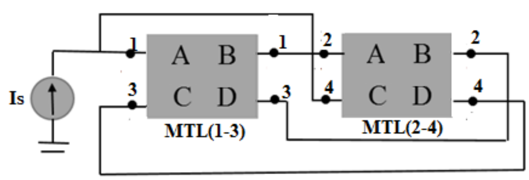

Fig. 4. Representation of two-port network for Fig. 2.

The above development is valid only for independent MTLs. However, for the two MTLs in Fig. 4, the following relations between currents and voltages can be established:

$$V_{s1} = V_{s4}, V_{r1} = V_{s2}, V_{r2} = V_{r3}, V_{s3} = V_{r4}, \tag{12}$$

$$I_s = I_{s1} + I_{s4}, I_{r1} = -I_{s2}, I_{r2} = -I_{r3}, I_{s3} = -I_{r4}. \tag{13}$$

By adding row 5 to 3, 7 to 4, 8 to 2 and 6 to 1 in (8), as well as applying (12) and (13), the following systems of equations is obtained:

$$\begin{bmatrix} V_{s1} \\ V_{s2} \\ V_{r3} \\ V_{r4} \end{bmatrix} = \begin{bmatrix} \bullet & \bullet & \bullet & \bullet \\ \bullet & \bullet & \bullet & \bullet \\ \bullet & \bullet & \bullet & \bullet \\ \bullet & \bullet & \bullet & \bullet \end{bmatrix}^{-1} \begin{bmatrix} I_s \\ 0 \\ 0 \\ 0 \end{bmatrix}. \tag{14}$$

Where "dots" in (14) indicate that these locations are filled with elements resulting from adding rows and columns. Also, the current source I_s in Fig. 4 represents the lightning current.

A. Improved MTL

The proposed MTL in the previous section is valid when ionization of soil is ignored. When, the electric field around the soil is greater than its critical value (E_c), ionization takes place. Such phenomenon is usually represented as gradually increasing radius of the electrode as shown in Fig. 5 (a). Hence, an improvement on the MTL is applied to a grounding electrode buried in an ionized soil as follows. Extension to grounding grids is straightforward.

Assume an electrode buried in a soil having conductivity of σ and dielectric constant of ε. Then divide it into N elemental conductors/segments which each one has radius of a_k and length of l_k. As shown in Fig. 5 (b), each segment can be represented as a two-port network.

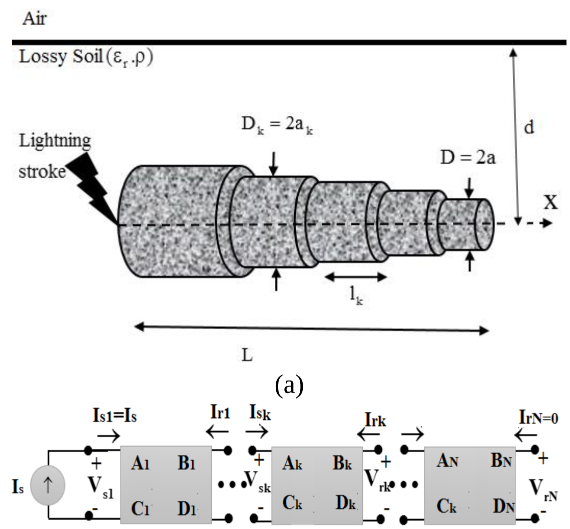

(b)

Fig. 5. (a) Ionization representation as gradually increasing radius, and (b) representation of each segment as a two-port network.

As known, the amount of current density draining to the surrounding soil from each segment in the frequency domain is given by:

$$J_k = (\sigma + j\omega\varepsilon)E_k. \tag{15}$$

On the surface of k-th segment, the relation between leakage current I_{Lk} and current density J_k is given as:

$$J_k = \frac{I_{Lk}/l_k}{2\pi a_k}, \tag{16}$$

where I_k is computed via subtracting currents at the sending and receiving points of the k-th segment, i.e.,

$$I_{Lk} = I_{sk} - I_{rk}. \tag{17}$$

Note that, once (14) is solved, via (8) sending and receiving currents at each conductor are easily computed. Finally, leakage current at each conductor is computed via (17). Now applying (16) on (15), the electric field on the surface of k-th segment is easily computed, that is:

$$E_k = \frac{J_k}{\sigma + j\omega\varepsilon} = \frac{I_{Lk}/l_k}{2\pi(\sigma + j2\pi f\varepsilon)a_k}, \quad k = 1,2,..,N \cdot \quad (18)$$

Then if the value of E_k is greater than the value of E_c, radius of each segment is increased as below:

$$a_{new,k} = a\frac{|E_k|}{E_c}, \quad k = 1,2...,N \cdot \quad (19)$$

In (19), a is the original radius of the electrode. Then for the new value of radius, (14) is again solved. At the first stage of the iteration process for each segment, $a_k = a$. This process is continued up to $E_k < E_c$. When this condition is achieved, the sending voltage of each segment in time domain, $v_{sk}(t)$, is computed as follows,

$$v_{sk}(t) = \sum_{m=1}^{M} V_{sk,m} \cos(2\pi f_m t + \phi_{sk,m}), \quad (20)$$

where M denotes the total number of selected frequency components of lightning current waveform. Also, $V_{sk,m}, \phi_{sk,m}$ are respectively magnitude and phase of sending voltage of k-th segment. Further information about modeling process for grounding grids of arbitrary size can be found in [23].

III. MODEL EVALUATION AND SIMULATION RESULTS

To examine the performance (accuracy and computation efficiency) of the proposed method, various cases have been investigated. For brevity, we study different cases for which the results are available in the literature. These case studies include soil ionization and dispersion separately or simultaneously. We then perform a sensitivity analysis where the effects of soil dispersion and ionization on transient analysis of a buried electrode will be studied.

To take into account soil dispersion, the expression proposed in [16] is used for calculating the effective permittivity and conductivity, i.e.,

$$\sigma(f) = \sigma_0\left(1 + \left(1.2.10^{-6}.\sigma_0^{-0.73}\right)(f - 100)^{0.65}\right), \quad (21)$$

$$\varepsilon_r(f) = \begin{cases} 192.2 & f \le 10\text{kHz} \\ 1.3 + 7.6.10^3.f^{-0.4} & f \ge 10\text{kHz} \end{cases}, \quad (22)$$

where σ_0 is the low-frequency conductivity of soil.

A. Accuracy

In the first case study, validity of the proposed approach in considering dispersion of soil is investigated. Hence, a vertical rod having length of L=3m, radius of a=12.5mm is selected. This rod is injected by first stroke current with peak value of 30kA, zero-to-peak time of $8\mu s$ and maximum steepness of $40kA/\mu s$. Grounding potential rise (GPR) for the two values of soil conductivity of $\sigma_0 = 0.001$, 0.0005 S/m are shown in Fig. 6. The results are compared with those obtained using the finite element method (FEM) [15], as a reference solution. A comparison of the results in this figure confirms the accuracy of the proposed method.

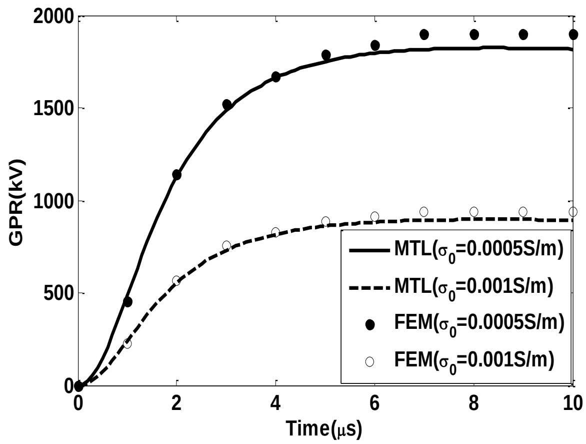

Fig. 6. Comparison of GPRs based on MTL and FEM [15] for validity in only-dispersive soils.

In the second example, capability of the MTL in only-ionized soils is investigated. To this aim, another case study carried out by measurement is selected from [24] and compared with the MTL. In this case, a horizontal electrode of length l=5m, radius a=4mm buried in depth of d=0.6m in soil with $\rho = 42\Omega.m$ and $\varepsilon_r = 10$ with $E_c = 350\,kV/m$ is considered. The GPRs computed by measurement and MTL are shown in Fig. 7 which are in good agreement with each other.

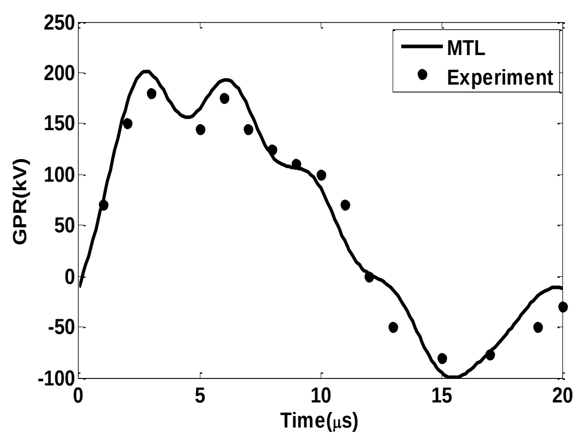

Fig. 7. Comparison of GPRs using MTL and measurement for validity in an only-ionized soil.

In another example to show capability of the MTL in considering ionization and dispersion simultaneously, a horizontal electrode of length L=15m buried in a lossy soil with conductivity $\sigma_0 = 0.002\,\mathrm{S/m}$ is selected. The critical electric field of soil is assumed to be $E_c = 300\,\mathrm{kV/m}$, and the peak value of excitation pulse is 10kA. As shown in Fig. 8, once more excellent agreement with the results in [13] are depicted. Note that for clarity of Fig. 8, situations of only-ionization and only-dispersion are not included.

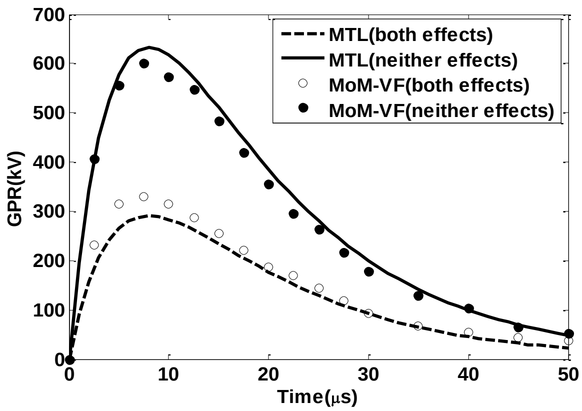

Fig. 8. Comparison of MTL-based GPRs with the MoM-VF results in [13] for validity.

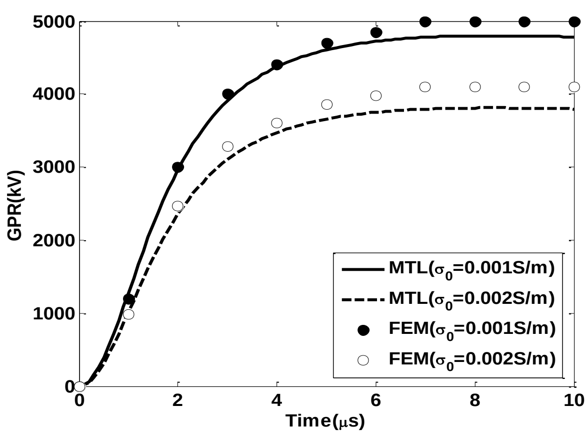

Fig. 9. Comparison of GPRs of the grounding grid by the MTL with FEM [15] for validity in an only-dispersive soil.

Finally, to show capability of the proposed model in considering mutual coupling between conductors, a grounding grid adopted from [15], is selected. The grid is an equally 2m×3m square and buried in depth of 0.5m inside a dispersive soil. The injection current is the same as the first example. The computed GPRs using FEM and MTL for $\sigma_0 = 0.001$, 0.002 S/m are computed and shown in Fig. 9. This figure shows that the results of the MTL are in good agreement with FEM [15].

B. Computational efficiency

In this section, to further show the accuracy of the MTL in comparison with the accurate models, a number of comparative data on the peak values of the GPRs and grounding resistances (R) in four situations, i.e., neither effects, only ionization, only dispersion and both effects, from the third example are listed in Table 1.

Table. 1: Comparison of peak values of GPRs and grounding resistances in different situations

Situation	**Neither Effects**		**Only Ionization**	
Method	MTL	[13]	MTL	[13]
GPR(kV)	615	605	300	310
R (Ω)	61.5	60.5	33	33.5
Situation	**Only Dispersion**		**Both Effects**	
Method	MTL	[13]	MTL	[13]
GPR(kV)	580	571	300	310
R (Ω)	58	57.1	30	31

The results in this table show good agreement with the ones in the published papers. The small differences in each situation in Table 1 undershoot might be due to the numerical errors introduced through the Fourier series that is used to obtain the time domain waveform of the lightning currents. Moreover, to show further efficiency of the MTL, the run-time of the MTL in computing GRRs for the different situations are listed in Table 2 which are very short in comparison with FEM and MoM. All computations were carried out on an Intel (R) Core (TM) i7-4702MQ CPU with 4GB of Ram.

Table 2: Approximate computation time of GPRs by different modeling approaches for the third example

Situation / Method	**Neither Effects**	**Only Ionization**
MTL	1 sec	1.4 sec
MoM FEM	258 sec 27.5 min	Not applicable Not applicable
Situation / Method	**Only Dispersion**	**Both Effects**
MTL	1.26 sec	1.5 sec
MoM FEM	174 sec 19.3 min	Not applicable Not applicable

IV. CONCLUSION

In this article, an efficient approach namely improved MTL was proposed in transient analysis of grounding electrodes considering ionization and dispersion of soil separately and simultaneously. This approach in despite of the approximate methods, can consider dispersion and ionization simultaneously, and coupling between parallel conductors is easily included as well. Moreover, its computational efficiency in contrast with numerical methods is considerably high. Extending the MTL for multilayer soils [25] is in progress.

REFERENCES

[1] *IEEE Guide for Safety in AC Substation Grounding*, IEEE Std. 80, Jan. 2000.

[2] *IEEE Recommended Practice for Grounding of Industrial and Commercial Power Systems (IEEE Green Book)*, IEEE Std. 142, 1991.

[3] C. M. Portela, M. C. Tavaras, and P. Filho, "Accurate representation off soil behavior for transient studies," *IEEE Proceedings of Generation, Transmission and Distribution*, vol. 150, no. 6, Nov. 2003.

[4] O. Goni, E. Kaneko, and A. Ametani, "Finite difference time domain method for the analysis of transient grounding resistance of buried thin wires," *Applied Computational Electromagnetic Society Journal (ACES)*, vol. 22, no. 3, pp. 42-49, 2007.

[5] Z. Feng, X. Wen, X. Tong, H. Lu, L. Lan, and P. Xing, "Impulse characteristics of tower grounding devices considering soil ionization by the time-domain difference method," *IEEE Transactions on Power Delivery*, vol. 30, no. 4, pp. 1906-1913, Aug. 2015.

[6] A. Habjanic and M. Trlep, "The simulation of the soil ionization phenomenon around the grounding system by the finite element method," *IEEE Transactions Magnetics*, vol. 42, no. 4, pp. 867-870, Apr. 2006.

[7] L. Qi, X. Cui, Z. Zhao, and H. Li, "Grounding performance analysis of the substation grounding grids by finite element method in frequency domain," *IEEE Transactions Magnetics*, vol. 43, no. 4, pp. 1181-1184, Apr. 2007.

[8] K. Sheshyekani, S. H. H. Sadeghi, R. Moini, and F. Rachidi, "Frequency-domain analysis of ground electrodes buried in an ionized soil when subjected to surge currents: A MoM–AOM approach," *Electric Power System Research*, vol. 81, pp. 290-296, 2011.

[9] J. C. Salari and C. Portela, "Grounding systems modeling including soil ionization," *IEEE Transactions on Power Delivery*, vol. 23, no. 4, pp. 1939-1949, Oct. 2008.

[10] J. Cidrás, A. F. Otero, and C. Garrido, "Nodal frequency analysis of grounding systems considering the soil ionization effect," *IEEE Transactions on Power Delivery*, vol. 15, no. 1, pp. 103-107, Jan. 2000.

[11] B. Zhang, J. He, J. Lee, X. Cui, Z. Zhao, and J. Zou, "Numerical analysis of transient performance of grounding systems considering soil Ionization by coupling moment method with circuit theory," *IEEE Transactions on Magnetics*, vol. 41, no. 5, pp. 1440-1443, May 2005.

[12] B. Zhang, J. Wu, Jinliang He, and R. Zeng, "Analysis of transient performance of grounding system considering soil ionization by the time domain method," *IEEE Transactions on Magnetics*, vol. 49, no. 5, pp. 1837-1840, Feb. 2013.

[13] J. Wu, B. Zhang, J. He, and R. Zeng, "A comprehensive approach for transient performance of grounding system in the time domain," *IEEE Transactions on Electromagnetic Compatibility*, vol. 57, no. 2, pp. 250-256, Apr. 2015.

[14] D. Cavka, N. Mora, and F. Rachidi, "A comparison of frequency-dependence soil models: application to the analysis of grounding systems," *IEEE Transactions on Electromagnetic Compatibility*, vol. 56, no. 1, pp. 177-187, 2014.

[15] M. Akbari, K. Sheshyekani, and M. R. Alemi, "The effect of frequency dependence of soil electrical parameters on the lightning performance of grounding systems," *IEEE Transactions on Electromagnetic Compatibility*, vol. 55, no. 4, pp. 739-746, Apr. 2013.

[16] S. Visacro and Rafael Alipio, "Frequency dependence of soil parameters: Experimental results, predicting formula and influence on the lightning response of grounding electrodes," *IEEE Transactions on Electromagnetic Compatibility*, vol. 27, no. 2, pp. 927-935, 2012.

[17] L. Grcev, "On high-frequency circuit equivalents of a vertical ground rod," *IEEE Transactions on Power Delivery*, vol. 20, no. 2, pp. 1598-1603, May 2009.

[18] L. Grcev, "On HF circuit models of horizontal grounding electrodes," *IEEE Transactions on Electromagnetic Compatibility*, vol. 20, no. 2, pp. 67-70, Aug. 2009.

[19] D. S. Gazzana, A. S. Bretas, G. A. D. Dias, M. Tello, D. W. P. Thomas, and C. Christopoulos, "The transmission line modeling method to represent the soil ionization phenomenon in grounding systems," *IEEE Transactions on Magnetics*, vol. 50, no. 2, pp. 1163-1171, Feb. 2014.

[20] A. F. Imece, D. W. Durbak, H. Elahi, S. Kolluri, A. Lux, D. Mader, T. E. McDermott, A. Morched, A. M. Mousa, R. Natarajan, L. Rugeles, and E. Tarasiewicz, "Modeling guidelines for fast front transients," *IEEE Transactions on Power Delivery*, vol. 11, no. 1, pp. 493-506, Jan. 1996.

[21] Y. Liu, M. Zitnik, and R. Thottappilli, "An improved transmission line model of grounding system," *IEEE Transactions on Electromagnetic Compatibility*, vol. 43, no. 3, pp. 348-355, Aug. 2001.

[22] Y. Liu, N. Theethayi, and R. Thottappilli, "An engineering model for transient analysis of grounding system under lightning strikes: Nonuniform transmission-line approach," *IEEE Transactions on Power Delivery*, vol. 20, no. 2, pp. 722-730,

Apr. 2005.

[23] A. Jardines, J. L. Guardado, J. Torres, J. J. Chavez, and M. Hernandez, “A multiconductor transmission line model for grounding grid,” *Electrical Power and Energy Systems*, vol. 60, pp. 24-33, Apr. 2014.

[24] A. Geri, “Behavior of grounding systems excited by high impulse currents: The model and its validation,” *IEEE Transactions on Power Delivery*, vol. 14, no. 3, pp. 1008-1017, July 1999.

[25] Z. Li, G. Li, J. Fan, and Y. Yin, “Numerical simulation of substation grounding grids buried in vertical earth model based on the thin-wire approximation with linear basis functions,” *Applied Computational Electromagnetic Society Journal (ACES)*, vol. 26, no. 4, pp. 32-39, 2011.